

Small-polaron transport and thermoelectric properties of the misfit-layer composite (BiSe)_{1.09}TaSe₂/TaSe₂

Jin Hee Kim,¹ Yoo Jang Song,¹ Jong-Soo Rhyee,^{1,*} Bong-Seo Kim,² Su-Dong Park,² Hyeung Jin Lee,³ and Jae-Wook Shin³

¹*Department of Applied Physics, Kyung Hee University, Yongin 446-701, Korea*

²*Advanced Electrical Materials Group, Korea Electrotechnology Research Institute, Changwon 641-600, Korea*

³*Lubricants Technology Laboratory, SK Innovation, Daejeon 305-712, Korea*

(Received 26 March 2013; revised manuscript received 8 May 2013; published 21 June 2013)

We studied the thermoelectric properties of the composite of misfit-layered compounds (BiSe)_{1.09}TaSe₂ and TaSe₂. The x-ray diffraction pattern on the cross-sectional plane of the sintered body shows a preferred orientation of the (00l) direction for (BiSe)_{1.09}TaSe₂/TaSe₂ indicating anisotropic alignment during hot pressing. Because of the crystallographic alignment, the temperature-dependent electrical resistivity $\rho(T)$, Seebeck coefficient $S(T)$, and the thermal conductivity $\kappa(T)$ exhibit in-plane and out-of-plane anisotropic transport behavior. The Seebeck coefficient is very low because of the coexistence of electron and hole mixing, as confirmed by the two-carrier model. The lattice thermal conductivity κ_L of the covalent bonding layer (in-plane) is lower than those of the layer with van der Waals bonding (out-of-plane) implying the existence of a charge density wave along the in-plane. We observed a sign anomaly of the positive Hall coefficient R_H and negative Seebeck coefficient S . According to Holstein's small-polaron model, the sign anomaly may come from the odd number of small-polaron hopping sites.

DOI: 10.1103/PhysRevB.87.224305

PACS number(s): 72.15.Jf, 65.40.-b, 68.65.Cd

I. INTRODUCTION

Recent advances on thermoelectric energy conversion materials have mostly focused on low-dimensional nanostructured systems and the design of new materials.^{1,2} The main objective of research on thermoelectric materials is to increase the thermoelectric performance, which is characterized by the dimensionless figure of merit ($ZT = S^2\sigma T/\kappa$), where S , σ , T and κ are the Seebeck coefficient, electrical conductivity, absolute temperature, and thermal conductivity, respectively. Two decades ago, it was proposed that ZT can be significantly enhanced in a low-dimensional system, due to quantum confinement and phonon scattering.³⁻⁵ The concept was realized in the experiment of artificial superlattices.⁶⁻⁹ However, there have been difficulties in scaling up these processes for applications such as thermoelectric refrigerators or power generators.¹⁰

In order to realize low dimensionality in bulk materials, many efforts have been devoted to development of the synthesis process and materials. It has been proven that nanoparticle dispersion in a bulk composite is an effective way to decrease thermal conductivity.^{11,12} As a natural low-dimensional system, we employed the Peierls distortion in a previous study.¹³ The charge density wave (CDW) is very effective for lowering the thermal conductivity with a high Seebeck coefficient for the following reasons. First, the Peierls distortion is driven by the strong electron-phonon coupling in a quasi-one-dimensional electronic system, which shows natural nanowirelike characteristics for a high Seebeck coefficient. Second, the phonon softening decreases the phonon energy near the Peierls transition, and the lattice distortion (Peierls distortion) increases disorder in the materials, which results in low thermal conductivity. Third, when we control the electron-phonon coupling via controlling the carrier concentration, the energy gap can be tuned to maximize the power factor ($S^2\sigma$). An increase in the power factor has been observed near the CDW transition temperatures.¹⁴

Just as the Peierls distortion is a realization of one-dimensional nanostructure, the natural superlattice is a kind of bulk upscaling of an artificial superlattice. Misfit-layer compounds $(MX)_{1+x}(TX_2)_n$ ($M = \text{Pb, Bi, Sn, Sb, and rare-earth elements}$; $T = \text{transition metals}$; $X = \text{chalcogenides}$; $n = 1, 2, 3$) consist of alternate stacking layers of MX and TX_2 with superlattice-like structure.¹⁵ The multiple stacking of different layered materials induces out-of-plane phonon blocking of the materials, which is important for low thermal conductivity. An anisotropic texture with preferred orientation is observed in the x-ray diffraction analysis of the cross-sectional plane of a sintered body in misfit-layered compounds.¹⁶

As a natural superlattice-structured material, we synthesized a composite of (BiSe)_{1.09}TaSe₂/TaSe₂. The reported Seebeck coefficient of (BiSe)_{1.09}TaSe₂ misfit layer compound is low $-20 \mu\text{V/K}$ at room temperature.¹⁷ Previously, a CDW transition was observed in TaSe₂ compound at 122 K.¹⁸ We investigated the thermoelectric properties of the composite orthorhombic (BiSe)_{1.09}TaSe₂ and hexagonal TaSe₂.¹⁹ Interestingly, when we measured the Hall resistivity, a positive sign of the Hall coefficient was observed, which contrasts with the negative Seebeck coefficient. Many misfit-layered compounds show sign mismatch in the Hall and Seebeck coefficients.¹⁵ Previous studies explained this behavior by light hole and heavy electron transport.¹⁷ However, there has been no clear evidence for different conduction mechanisms. We examined the mobilities of electrons and holes in terms of a two carrier model, and found that the sign mismatch in the Hall and Seebeck coefficients may come from the existence of an odd number of small-polaron hopping sites.²⁰

II. EXPERIMENT

The (BiSe)_{1.09}TaSe₂/TaSe₂ composite was synthesized in a solid-state reaction from the stoichiometric mixture of Bi (99.999%, lump), Se (99.999%, granule), and Ta (99.9%,

powder). The elements were sealed in an evacuated quartz tube and heated at 773 K and 1,073 K for 12 h and 24 h, respectively. The melted ingot was pulverized and vacuum sealed again. The powder was heat treated at 973 K for 48 h and water quenched. The compound was pulverized again and sintered by spark plasma sintering (SPS) under uniaxial pressure of 50 MPa at 973 K for 5 min. The x-ray diffraction (XRD) measurement were performed using Cu $K\alpha$ radiation (D8 Advance, Bruker) before and after SPS. The electrical resistivity ρ and Seebeck coefficient S were measured using a thermoelectric measurement system (ZEM-3, ULVAC, Japan). The Hall resistivity ρ_{xy} was measured using the five-probe contact method under a sweeping magnetic field ranging from 1 T to 5 T using the physical property measurement system (PPMS, Quantum Design, USA). The thermal conductivity was obtained by the relation $\kappa = \rho_s C_p \lambda$ where κ , ρ_s , C_p , and λ are the thermal conductivity, sample density, specific heat, and thermal diffusivity, respectively. The thermal diffusivity was measured using the laser flash method (LFA-447, NETZSCH, Germany).

III. RESULTS AND DISCUSSION

Figure 1 shows the XRD pattern of the powder sample of the $(\text{BiSe})_{1.09}\text{TaSe}_2/\text{TaSe}_2$ composite before spark plasma sintering. The powder XRD pattern was almost identical to the XRD pattern of the cross-sectional plane of the sintered sample. The main peaks are hexagonal TaSe_2 and face centered orthorhombic $(\text{BiSe})_{1.09}\text{TaSe}_2$ with crystallographical c -axis $(00l)$ alignment. Minor $(20l)$ peaks are observed in $(\text{BiSe})_{1.09}\text{TaSe}_2$. The lattice parameters of $(\text{BiSe})_{1.09}\text{TaSe}_2$ and the TaSe_2 compounds are shown in Table I, and are consistent with other reported data.²¹ The preferred orientation along the $(00l)$ -direction has significant importance for thermoelectric applications. From many reported papers, we argued that the intrinsic low dimensionality such as the Peierls distortion and charge density wave have an effect of lowering the thermal conductivity with a high Seebeck coefficient.^{13,14,22,23} In order to obtain low dimensionality in bulk materials, single crystals

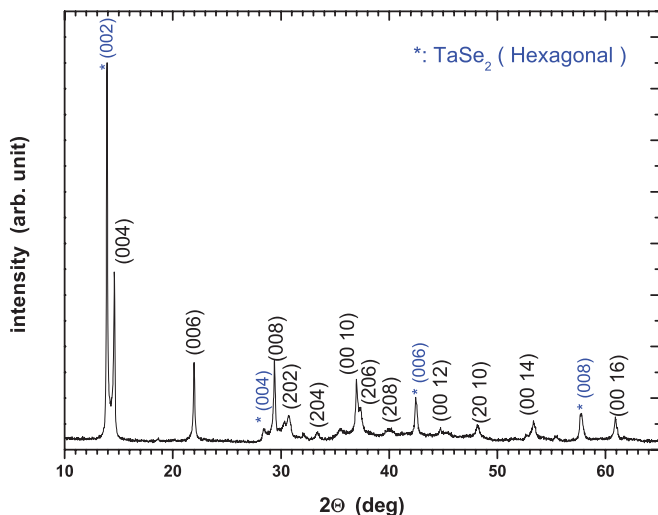


FIG. 1. (Color online) The power x-ray diffraction pattern of $(\text{BiSe})_{1.09}\text{TaSe}_2/\text{TaSe}_2$ composite.

TABLE I. The lattice parameters of $(\text{BiSe})_{1.09}\text{TaSe}_2$ and TaSe_2 .

structure	BiSe orthorhombic	TaSe_2 orthorhombic	TaSe_2 hexagonal
a (Å)	5.9913	5.9913	3.4563
b (Å)	6.2627	3.4162	3.4563
c (Å)	24.2758	24.2758	12.7648

should be grown, which are expensive, and the process is time consuming. The texture with c -axis alignment in a bulk-sintered ingot is important for mass production of the materials with low-dimensional anisotropic transport properties.

Figure 2 presents the temperature-dependent anisotropic thermoelectric properties of the $(\text{BiSe})_{1.09}\text{TaSe}_2/\text{TaSe}_2$ composite. The in-plane and out-of-plane electrical resistivity $\rho(T)$ shows metallic behavior, as shown in Fig. 2(a). Due to the van der Waals bonding along the c -axis direction of the misfit-layered compound, the $\rho(T)$ of in-plane (~ 0.22 m Ω -cm) is lower than the out-of-plane (~ 0.47 m Ω -cm) at 325 K. The in-plane resistivity of our sample is similar to that of the powder pelletized compacts of $(\text{BiSe})_{1.09}\text{TaSe}_2$ presented by Zhou *et al.* (~ 0.24 m Ω -cm at 300 K)¹⁷ and Oosawa *et al.* (~ 2.2 m Ω -cm at 280 K).¹⁹ Because the electrical resistivity of TaSe_2 is very low (~ 1.2 $\mu\Omega$ -cm at 280 K),²⁴ we believe that the dominant contribution of $\rho(T)$ comes from the $(\text{BiSe})_{1.09}\text{TaSe}_2$ misfit-layered compound.

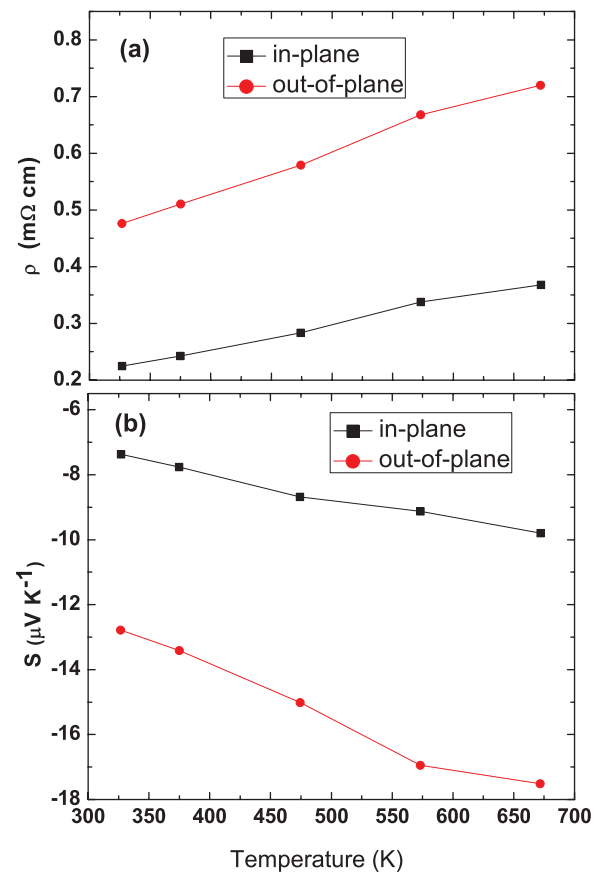


FIG. 2. (Color online) Temperature-dependent in-plane and out-of-plane electrical resistivity ρ (a), Seebeck coefficient S (b) of $(\text{BiSe})_{1.09}\text{TaSe}_2/\text{TaSe}_2$ composite.

The Seebeck coefficient $S(T)$ is negative, as shown in Fig. 2(b), indicating that the main charge carriers are electrons. The anisotropic Seebeck coefficient $S(T)$ shows very low values for the in-plane ($\sim -7.4 \mu\text{V K}^{-1}$) and out-of-plane directions ($\sim -12.8 \mu\text{V K}^{-1}$) at 325 K. The low Seebeck coefficient may be affected by two types of carriers because the Seebeck coefficients of electrons S_e and holes S_h can be compensated for by the following equation:

$$S = \frac{\sigma_e S_e + \sigma_h S_h}{\sigma_e + \sigma_h}, \quad (1)$$

where σ_e and σ_h are the electrical conductivities of electrons and holes, respectively.³

To confirm the possibility of electron and hole mixing, we analyzed the Hall mobility of holes (μ_h) and electrons (μ_e) using a two-carrier model calculated by the following relations:²⁵

$$R_H = \frac{\mu_h - \mu_e}{ne(\mu_h + \mu_e)} \quad (2)$$

$$\frac{\Delta\rho}{\rho} = \frac{\rho(H) - \rho(0)}{\rho(0)} = \mu_e \mu_h H^2 \quad (3)$$

$$\sigma = 1/\rho = ne(\mu_e + \mu_h), \quad (4)$$

where R_H , ρ , H , $\mu_{e(h)}$, and n are Hall coefficient, electrical resistivity, magnetic field, Hall mobility of electron (hole), and carrier density, respectively. Here we assumed that the carrier densities of electron and hole are identical. The calculation results are presented in Table II. The in-plane mobilities of holes and electrons are slightly higher than the out-of-plane mobilities, which is consistent with the van der Waals bonding along the c direction. The identical mobilities of holes μ_h and electrons μ_e clearly shows two types of the carriers. So, it can be understood that the cause of low Seebeck coefficient of the $(\text{BiSe})_{1.09}\text{TaSe}_2/\text{TaSe}_2$ composite mainly originates from the electron-hole mixing of carriers.

The total thermal conductivity is composed of the electronic κ_{el} and the lattice thermal conductivity κ_L . The electronic thermal conductivity κ_{el} can be calculated by the Wiedemann-Franz law $\kappa_{\text{el}} = L_0 \sigma T$ where L_0 , σ , and T are the Lorenz number, electrical conductivity, and absolute temperature, respectively. In usual cases, the Lorenz number is written as

$$L_0 = \frac{\pi^2}{3} \left(\frac{k_B}{e} \right)^2 = 2.45 \times 10^{-8} \text{W}\Omega \text{K}^{-2}. \quad (5)$$

However, the Lorenz number is incorrect in correlated metal and many degenerated semiconductors. In order to obtain

TABLE II. The calculated parameters of in-plane and out-of-plane Hall coefficient R_H , electronic Hall mobility μ_e , Hall mobility of holes μ_h , and Hall carrier density n_H of $(\text{BiSe})_{1.09}\text{TaSe}_2/\text{TaSe}_2$ composite.

	R_H (m^3/C)	μ_e ($\text{mm}^2 \text{V}^{-1} \text{s}^{-1}$)	μ_h ($\text{mm}^2 \text{V}^{-1} \text{s}^{-1}$)	n_H (cm^{-3})
at 300 K				
in-plane	1.0×10^{-9}	454.1586	454.1587	1.1×10^{21}
out-of-plane	3.7×10^{-9}	417.5721	417.5719	4.3×10^{20}

reliable lattice thermal conductivity, we should examine the temperature-dependent Lorenz factor by the relation as follows:²⁶

$$L = \left(\frac{k_B}{e} \right)^2 \left(\frac{(r+7/2)F_{r+5/2}(\eta)}{(r+3/2)F_{r+1/2}(\eta)} - \left[\frac{(r+5/2)F_{r+3/2}(\eta)}{(r+3/2)F_{r+1/2}(\eta)} \right]^2 \right), \quad (6)$$

where r is the scattering parameter and $\eta = E_F/k_B T$ is the reduced Fermi energy. In most cases, the scattering parameter of acoustic phonon scattering is $r = -1/2$. So, prior to calculate Lorenz factor, we should obtain the reduced Fermi energy η by fitting the Seebeck coefficient from Fig. 2(b) as following equation:

$$S = \pm \frac{k_B}{e} \left(\frac{(r+5/2)F_{r+3/2}(\eta)}{(r+3/2)F_{r+1/2}(\eta)} - \eta \right), \quad (7)$$

where $F_n(\eta)$ is the n th order Fermi integral,

$$F_n(\eta) = \int_0^\infty \frac{x^n}{1 + e^{x-\eta}} dx. \quad (8)$$

Using the above equation, we can get the Fermi integral in terms of the reduced Fermi energy. The calculated temperature-dependent Lorenz number is depicted in Fig. 3(a). The in-plane Lorenz number is temperature insensitive with a factor of $2.43 \sim 2.44 \times 10^{-8} \text{W}\Omega \text{K}^{-2}$, which is slightly

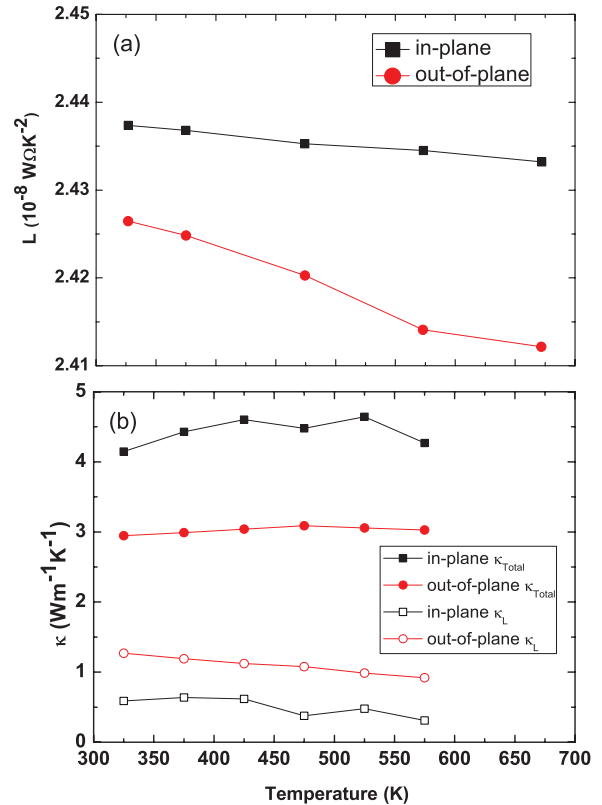


FIG. 3. (Color online) Temperature-dependent in-plane and out-of-plane Lorenz factor obtained by Eqs. (6) and (7). (a) (see in the text) and total κ_{tot} (closed symbols) and lattice thermal conductivity κ_L (open symbols) (b) of $(\text{BiSe})_{1.09}\text{TaSe}_2/\text{TaSe}_2$ composite.

lower than the conventional Lorenz number $L_0 = 2.45 \times 10^{-8} \text{ W}\Omega \text{ K}^{-2}$. The out-of-plane Lorenz number is much lower than L_0 and decreases with increasing temperature from $2.427 \times 10^{-8} \text{ W}\Omega \text{ K}^{-2}$ at 325 K to $2.412 \times 10^{-8} \text{ W}\Omega \text{ K}^{-2}$ at 675 K. The anisotropic Lorenz factor indicates the different chemical potential for different orientations of in-plane and out-of-plane directions.

Figure 3(b) shows the total thermal conductivity $\kappa_{\text{tot}}(T)$ (closed symbols) and lattice thermal conductivity $\kappa_L(T)$ (open symbols) of the $(\text{BiSe})_{1.09}\text{TaSe}_2/\text{TaSe}_2$ composite. The thermal conductivities are almost insensitive to temperature throughout the temperature range from 325 K to 575 K. The in-plane total thermal conductivity ($\sim 4.1 \text{ W m}^{-1} \text{ K}^{-1}$) is higher than the out-of-plane total thermal conductivity ($\sim 2.9 \text{ W m}^{-1} \text{ K}^{-1}$) at 325 K. Because we obtain the temperature-dependent anisotropic Lorenz factor, we can obtain the lattice thermal conductivity κ_L by subtraction of the electronic thermal conductivity κ_{el} , as shown in Fig. 3(b) (open symbols). Interestingly, the in-plane lattice thermal conductivity is lower than the out-of-plane conductivity. This behavior is not consistent with other misfit-layer compounds¹⁶ and is contrary to our expectations, because the misfit-layer compound has layered structure with van der Waals bonding along the c direction. It was reported that the TaSe_2 compound showed a charge density wave (CDW) transition at 122 K.¹⁸ Thus, we anticipate that phonon softening may have participated by strong electron-phonon coupling. The lower lattice thermal conductivity of a covalent bonding layer than those of the van der Waals bonding layer can be enabled by the phonon softening upon the CDW formation.¹³ However, the measurement range in this case is higher than the CDW transition temperature. The possibility of CDW formation in the misfit-layered compound $(\text{BiSe})_{1.09}\text{TaSe}_2$ should be investigated in further work.

From the measurement of the Hall resistivity ρ_{xy} , we obtained the Hall coefficient $R_H = \rho_{xy}/H$ under a magnetic field of $H = 1 \text{ T}$ as depicted in Fig. 4(a). The Hall coefficient is positive over the entire measured temperature range, from 2 K to 200 K. Noting that the Seebeck coefficient is negative, the positive Hall coefficient does not match with the negative Seebeck coefficient. This unusual phenomenon was also observed previously for $(\text{BiSe})_{1.09}\text{TaSe}_2$ ¹⁷ and some other misfit-layered compounds.¹⁵ It has been reported that the Hall sign anomaly is due to the heavy electron and light hole transport.¹⁷ However, there is no convincing evidence of the argument based on the electronic band structure calculation. If we assume the asymmetric bands from heavy electron and light hole, it is not consistent with the significantly low Seebeck coefficient and almost identical electron and hole mobilities obtained by two carrier model. The almost identical electron and hole mobilities can describe well the origin of low Seebeck coefficient, which indicate that the heavy electron and light hole argument is unlikely.

The sign anomaly between the Hall and Seebeck coefficients can be caused by several scenarios, such as the anomalous Hall effect induced by skew scattering and side-jump, Umklapp scattering in a high magnetic field,²⁷ and small-polaron transport. In the field-dependent Hall resistivity ρ_{xy} measurements, we did not observe an anomalous Hall effect. Second, the Hall coefficient sign change by the Umklapp

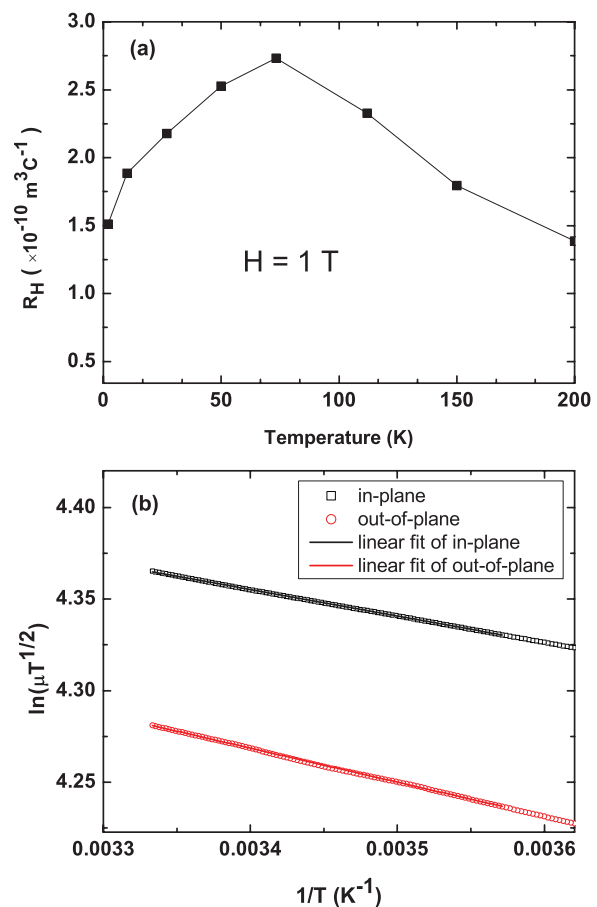


FIG. 4. (Color online) Temperature-dependent Hall coefficient R_H under a magnetic field of $H = 1 \text{ T}$ (a) and the linear fitting result of in-plane and out-of-plane Hall mobilities in terms of the three-site polaronic hopping model of $(\text{BiSe})_{1.09}\text{TaSe}_2/\text{TaSe}_2$ composite.

process by intersheet scattering between Fermi surfaces is unlikely, because the Hall sign change is field-dependent in the case of intersheet scattering, but the sign of R_H is field insensitive under various magnetic fields in our measurement (not shown). The last possibility of the Hall sign anomaly is the small-polaron transport. The electron path under a magnetic field experiences the Aharonov-Bohm effect. In this case, the sign of the Hall angle is determined by the sign of the products of electronic transfer integrals $J_{i,i+1}$ between i and the nearest-neighbor site $i + 1$, according to the following equation:²⁸

$$\text{sign}(\theta_{\text{Hall}}) = \text{sign} \left[\epsilon^{n+1} (-q) (-1)^n \prod_{i=1}^n J_{i,i+1} \right] \quad (9)$$

where $\epsilon = 1$ for electrons and $\epsilon = -1$ for holes and n is the number of small-polaron hopping sites. For odd-number of small-polaron hopping sites, the three-site electron hopping between orbitals gives rise to the positive Hall sign angle. The sign mismatch between the Hall and Seebeck coefficients by the odd-numbered leg of small polarons was observed in p -type manganites, where R_H is negative and S is positive.²⁰

In order to speculate on the existence of small polarons, we examined the Hall mobility in terms of three-site hopping (Eq. 10) and four-site hopping (Eq. 11) of polarons according to the following equations:

$$\mu_H \propto \left(\frac{\hbar\omega_0}{k_B T} \right)^{\frac{1}{2}} \exp \left(-\frac{W_H}{k_B T} \right) \quad (10)$$

$$\mu_H \propto \left(\frac{\hbar\omega_0}{k_B T} \right)^{\frac{3}{2}} \exp \left(-\frac{1}{3} \frac{W_H}{k_B T} \right), \quad (11)$$

where μ_H , W_H , and ω_0 are the Hall mobility, hopping activation energy, and longitudinal optical phonon frequency, respectively. Figure 4(b) shows the fitting results of the calculated mobilities of the in-plane and out-of-plane directions obtained by the three-site hopping polaron model. The mobility μ_H from the value obtained from the two-band model is used. The three-site hopping gives more reasonable fitting results than those of four-site hopping from 270 K to 300 K, as shown in Fig. 4(b). The fitted activation energy W_H of three-site hopping is about 3.76 eV for in-plane and 4.9 eV for out-of-plane. The higher activation energy of out-of-plane is reasonable, because of the weak van der Waals bonding along the c axis.

The interpretation of the small-polaron model can be justified by the possible existence of a charge density wave in the quasi-two-dimensional structure of a misfit-layered compound. The small-polaron and charge density wave are commonly caused by strong electron-phonon coupling. Based on the lattice thermal conductivity κ_L in Fig. 3(b), the lower lattice thermal conductivity along the in-plane than along the out-of-plane might be due to the charge density wave. Because the TaSe₂ exhibits CDW, the TaSe₂ layer in the misfit-layered compound (BiSe)_{1.09}TaSe₂ can have strong electron-phonon coupling. The strong electron-phonon coupling in the materials

system can be justified by the existence of the small-polaron transport.

IV. CONCLUSION

In summary, we have synthesized a (BiSe)_{1.09}TaSe₂/TaSe₂ composite by a simple solid-state reaction with (001) preferred orientation. The natural texturing along the c axis might have great importance for practical thermoelectric applications of low-dimensional electronic system, such as charge density waves. This composite exhibits anisotropic thermoelectric properties even in the polycrystalline materials due to the anisotropic texture. In spite of a low Seebeck coefficient by electron-hole mixing confirmed by two-band model, the low-dimensional nature can be manifested in bulk polycrystalline materials. The lower in-plane lattice thermal conductivity than the out-of-plane lattice thermal conductivity implies the effect of charge density wave and/or strong electron-phonon coupling mechanism along the in-plane direction. From the Holstein's polaron model, the sign anomaly between R_H and S can be successfully understood by the three-site hopping of small polaron driven by the strong electron-phonon coupling.

ACKNOWLEDGMENTS

This research was supported by the Basic Science Research Program through the National Research Foundation of Korea (NRF) funded by the Ministry of Education, Science and Technology (Grants No. 2011-0021335 and No. 2012R1A2A1A03005174), as well as a grant from the Energy Efficiency & Resources program of the Korea Institute of Energy Technology Evaluation and Planning (KETEP) funded by the Korean government Ministry of Knowledge Economy (Grant No. 20112010100100), and from the SK Innovation.

*jsrhyee@khu.ac.kr

¹A. J. Minnich, M. S. Dresselhaus, Z. F. Ren, and G. Chen, *Energy Environ. Sci.* **2**, 466 (2009).

²J. R. Sootsman, D. Y. Chung, and M. G. Kanatzidis, *Angew. Chem. Int. Ed.* **48**, 8616 (2009).

³L. D. Hicks and M. S. Dresselhaus, *Phys. Rev. B* **47**, 12727 (1993).

⁴L. D. Hicks, T. C. Harman, X. Sun, and M. S. Dresselhaus, *Phys. Rev. B* **53**, R10493 (1996).

⁵M. S. Dresselhaus, G. Chen, M. Y. Tang, R. Yang, H. Lee, D. Wang, Z. Ren, J.-P. Fleurial, and P. Gogna, *Adv. Mater.* **19**, 1043 (2007).

⁶J. Yang and T. Caillat, *MRS Bull.* **31**, 224 (2006).

⁷R. Venkatasubramanian, E. Siivola, T. Colpitts, and B. OQuinn, *Nature (London)* **413**, 597 (2001).

⁸T. C. Harman, P. Taylor, M. P. Walsh, and B. E. LaForge, *Science* **297**, 2229 (2002).

⁹T. C. Harman, P. J. Taylor, D. L. Spears, and M. P. Walsh, *J. Electron. Mater.* **29**, L1 (2000).

¹⁰F. J. DiSalvo, *Science* **285**, 703 (1999).

¹¹K. F. Hsu, S. Loo, F. Guo, W. Chen, J. S. Dyck, C. Uher, T. Hogan, E. K. Polychroniadis, and M. G. Kanatzidis, *Science* **303**, 818 (2004).

¹²W. Kim, J. Zide, A. Gossard, D. Klenov, S. Stemmer, A. Shakouri, and A. Majumdar, *Phys. Rev. Lett.* **96**, 045901 (2006).

¹³J.-S. Rhyee, K. H. Lee, S. M. Lee, E. Cho, S. I. Kim, E. Lee, Y. S. Kwon, J. H. Shim, and G. Kotliar, *Nature (London)* **459**, 965 (2009).

¹⁴J. H. Kim, J.-S. Rhyee, and Y. S. Kwon, *Phys. Rev. B* **86**, 235101 (2012).

¹⁵J. Rouxel, A. Meerschaut, and G. A. Wieggers, *J. Alloys Comp.* **229**, 144 (1995).

¹⁶C. Wan, Y. Wang, N. Wang, W. Norimatsu, M. Kusunoki, and K. Koumoto, *J. Electron. Mater.* **40**, 1271 (2011).

¹⁷W. Y. Zhou, A. Meetsma, J. L. de Boer, and G. A. Wieggers, *Mater. Res. Bull.* **27**, 563 (1992).

¹⁸B. Dardel, M. Grioni, D. Malterre, P. Weibel, Y. Baer, and F. Levy, *J. Phys.: Condens. Matter* **5**, 6 (1993).

¹⁹Y. Oosawa, J. Akimoto, M. Sohma, T. Tsunoda, H. Hayakawa, and M. Onoda, *Solid State Ionics* **101**, 9 (1997).

²⁰M. Jaime, H. T. Hardner, M. B. Salamon, M. Rubinstein, P. Dorsey, and D. Emin, *Phys. Rev. Lett.* **78**, 951 (1997).

²¹Y. Oosawa, Y. Gotoh, J. Akimoto, and M. Onoda, *J. Alloys Comp.* **176**, 319 (1991).

- ²²J.-S. Rhyee, E. Cho, K. H. Lee, S. I. Kim, E. S. Lee, S. M. Lee, and Y. S. Kwon, *J. Appl. Phys.* **105**, 053712 (2009).
- ²³K. E. Lee, B. H. Min, J.-S. Rhyee, J. N. Kim, J. H. Shim, and Y. S. Kwon, *Appl. Phys. Lett.* **101**, 143901 (2012).
- ²⁴H. N. S. Lee, M. Garcia, H. Mckinzie, and A. Wold, *J. Solid State Chem.* **1**, 190 (1970).
- ²⁵B. Sapoval and C. Hermann, *Physics of Semiconductors* (Springer-Verlag, New York, 1988).
- ²⁶W.-S. Liu, Q. Zhang, Y. Lan, S. Chen, X. Yan, Q. Zhang, H. Wang, D. Wang, G. Chen, and Z. F. Ren, *Adv. Energy Mater.* **1**, 577 (2011).
- ²⁷C. L. Chien, *The Hall Effect and its Applications* (Plenum Press, New York, 1980).
- ²⁸D. Emin, *Philos. Mag.* **35**, 1189 (1977).